International Journal of Mechanical and Materials Engineering (IJMME), Vol. 4 (2009), No. 1, 24 -34.

PERFROMANCE OF AN IMPROVED SOLAR CAR VENTILATOR

R. Saidur, H. H. Masjuki and M. Hasanuzzaman
Department of Mechanical Engineering
University of Malaya, 50603 Kuala Lumpur, Malaysia
E-mail: hasan492@yahoo.com

ABSTRACT

The ventilator inhales fresh air from outside into the inside cabin of a vehicle and exhales hot air to the outside. On a sunny day, solar energy can be used to run the ventilator, and to charge the battery simultaneously. During a cloudy day, the ventilator can be driven by the battery. In this paper, heat transfer and energy balance inside the car were investigated. Moreover power consumption of the motor, power produced from the solar panel, radiation effect and battery charging time were investigated. The present study suggests that the motor in the existing ventilator should be replaced by a high speed motor. It is found that more electricity is needed for high speed motor in an improved ventilator. In this paper, a commercially available ventilator has been modified to improve its performance. The modification has increased air flow rate from 20 cfm to 110.5 cfm. The improved ventilator provided at least 11% better result of reducing the temperature inside a car compared to the existing one.

Keywords: Ventilator; Radiation; Energy; Solar panel.

1. INTRODUCTION

In modern era, most people drive cars and during driving sometimes the cars are needed to park in the open area where it is directly exposed to the sunlight. If the car is parked for too long time exposing the sunlight, the air inside the car becomes very hot. The temperature inside the car can easily rise to 60ºC. Even in fairly cloudy day, the temperature inside the car can easily reach 55 ºC. It is difficult to get on a car having exposed several hours to solar radiation. The hot temperature inside the car absolutely makes the driver feel uncomfortable in the first 10 minutes (Mezrhab and Bouzidi, 2005). In recent years, many works were reported on thermal comfort inside a car (Bureau *et al.,* 2004; Martinho *et al.,* 2004; Farrington *et al.,* 1999; Jaksic *et al.,* 2003). In a sunny day, the conditions of comfort inside a car depend closely on the exchanges of thermal radiation between the vehicle and its environment as well as internal radiation inside the car compartment. The radiation is undoubtedly the most instantaneous phenomena of energy transfer. To convince one, it is sufficient to consider the immediate feeling or relief which one experiences when one takes a shady road after having driven a long time in a sunny day. The solar radiation heats up the equipment inside the car. These equipment will absorb heat and will make the car compartment hard to be cooled down within a short period of time. As a result, the driver needs to run the air-conditioning before starting to drive. This will increase the fuel consumption of the car (Jaksic *et al.,* 2003). If the thermal load on the passenger compartment can be reduced, the power consumption of an air conditioning (AC) compressor can be reduced as well. Consequently, a reduction in individual vehicle's fuel consumption could lead to enormous fuel savings worldwide (Farrington *et al.,* 1999). The potential technique for reducing fuel consumption of the car is to reduce the vehicle climate temperature. Minimizing the heat gain inside the car compartment by a ventilator was noted as an efficient method for reducing the soak temperature (Farrington *et al.,* 1999).

The glass absorbing the solar radiation will itself become a heat source. The amount of absorbed energy will determine the temperature of the glass and thus the direction of heat flow. The percentage of heat dissipated inside the vehicle can be determined by using the preliminary heat transfer analysis. The heat transfer analysis involves convection and radiation from the glass to the vehicle interior and to the outside air (Jaksic *et al.,* 2003). About 80% of the temperature inside the car compartment rises during the first 30 minutes. There was an average 4.4°C increase in temperature inside the car compartment for ambient temperature spanning 22.2°C to 35.6°C. In a sunny day, the temperature rise in vehicles was significantly clear even when the ambient temperature was not too hot (McLaren *et al.,* 2006). The heating process did not slow down and the maximum temperature did not decrease even with the windows leaving slightly opened (McLaren *et al.,* 2006). When the engine is started, an air conditioner cannot effectively adjust the temperature inside a car compartment within a short period. The engine can not provide the optimum working temperature; hence it leads to the heavy duty operation on the engine and increases the fuel consumption.

Reducing the climate control loads in a vehicle is important to improve vehicle's fuel economy (David Huang *et al.,* 2005). In the US, every year many children die of heat stroke after being left unattended in vehicles.

From the year 1998 to 2002, the average number of children died of heat stroke was 29 persons per year. In 2003, this number increased to 42 and 35 persons in 2004. Annually, hundreds of children experience varying degrees of heat illness from being left in cars (Mezrhab and Bouzidi, 2005). Hodder and persons (2007) investigated the relationship between simulated solar radiation and thermal comfort. The authors investigated the effects of (1) the intensity of direct simulated solar radiation, (2) spectral content of simulated solar radiation and (3) glazing type on human thermal sensation responses.

The literature review reveals that many researchers carried out CFD work (Mezrhab and Bouzidi, 2006; Kaynakli *et al.*, 2002). Intelligent solar-powered automobile-ventilation system was studied by David *et al.*, (2005). Mezrhab and Bouzidi (2006) developed a numerical model to study the behavior of thermal comfort inside the passenger car compartment according to climatic conditions and materials that compose the vehicle. Available thin films on the glass window can not maintain comfortable temperature inside the car compartment. This investigation also found that the existing ventilation is not enough to meet the required comfort. The main objectives of these work is to identify the key point of the vehicle compartment and placed the ventilator system for optimum performance. In addition, this work also attempts to improve the existing ventilator system and use the solar energy to run the ventilator. The ventilator was refurbished by using the solar controller, additional battery, and solar panel for uninterrupted running of the ventilator. A bigger motor was used to increase the air flow rate. The position of the existing ventilator's solar panel was not suitable because it was placed at the side of a car. As a result, the solar panel was not directly receiving the sunlight. In this experiment the solar panel was placed on the roof of the car to improve its efficiency to produce electricity.

2. RESEARCH METHODOLOGY

2.1 Existing car ventilator

The existing solar car ventilator shown in Figure 1 is run by solar energy. It can also be driven by energy supplied through the vehicle's battery. The ventilator can keep functioning when the vehicle is parked under the sunlight even if the vehicle engine is turned off since the ventilator is driven by the solar energy. When sunlight gets weak, the ventilator can be alternatively driven by energy supplied from the vehicle's battery. The battery can be charged using the sunlight. Table 1 shows the specification of the existing car ventilator.

(a) (b)

Figure 1 Existing solar car ventilator: (a) ventilator fan, (b) solar panel

Table 1 Specification of an existing solar car ventilator

Components	Capacity
Solar panel	1.2W per solar panel
Brushless DC motor	6 V/200mA
Flow rate	20cfm

2.2 Silicon solar panel

Monocrystalline solar cells shown in Figure 2 are connected in series to produce solar panels. As each cell produces a voltage between 0.5 and 0.6 volts, 36 cells are needed to produce an open-circuit voltage of about 20 volts. This is sufficient to charge a 12 volt battery. Table 2 shows the specification of the solar panel.

Figure 2 Monocrystalline silicon solar panel

Table 2 Specification of monocrystalline silicon solar panel

Specification	Rating
P_{max}	SW25
V_{mp}	18 volt
I_{mp}	1.39A
V_{oc}	21 V
I_{sc}	1.53A
Maximum system voltage	600 V
Size (mm)	536×446×35
Test conditions	AM1.5, 25 ^{0}C,1000W/m^2

2.3 Solar controller

A solar controller shown in Figure 3 is connected with the battery, improved ventilator, and solar panel. It provides energy to the improved ventilator and charges the battery at the same time.

Figure 3 Solar controller

It will stop further current flow into the battery when the battery is full. Solar controller stops charging a battery when it exceeds a set of high voltage level, and re-enables charging when the battery voltage drops below that level. Solar controller also acts as a power regulator. When the solar panel does not produce stable electricity, the solar controller will use the battery power to regulate the electricity so that the improved ventilator operates at maximum speed.

2.4 Improved solar car ventilator

It may be mentioned that the existing ventilator shown in Figure 1 can not remove heat from the interior cabinet of a vehicle effectively. In order to improve its performance, a bigger fan and motor have been proposed to replace the existing one. The fan was removed from the motor shaft and then the motor along with its platform was dismantled from the existing ventilator body. The fan was fixed with the motor shaft-lock of the ventilator. As the proposed motor's size was different, a new platform was built to accommodate the new motor. Existing fan was replaced by two CPU brushless DC fans. The new motor was placed at the centre of the front casing and maintained 5mm gap from the front casing to avoid collision. Before placing the motor, the motor legs were soldered with additional 1.5m stranded copper wires and then positive and negative wires were twisted together to avoid the wires being hit by the fan. These cables were then connected with the solar controller. The existing solar panel was removed and new solar panel was placed over the roof of the car as shown in Figure 6. An 18cm AR 17 steel band was used to hold the new motor. The steel band was bent according to the motor's shape after the motor was lifted 5mm and the motor was tied securely using cables and AR 17 steel band as shown in the figure. The improved solar car ventilator with the above modifications is shown in Figure 4.

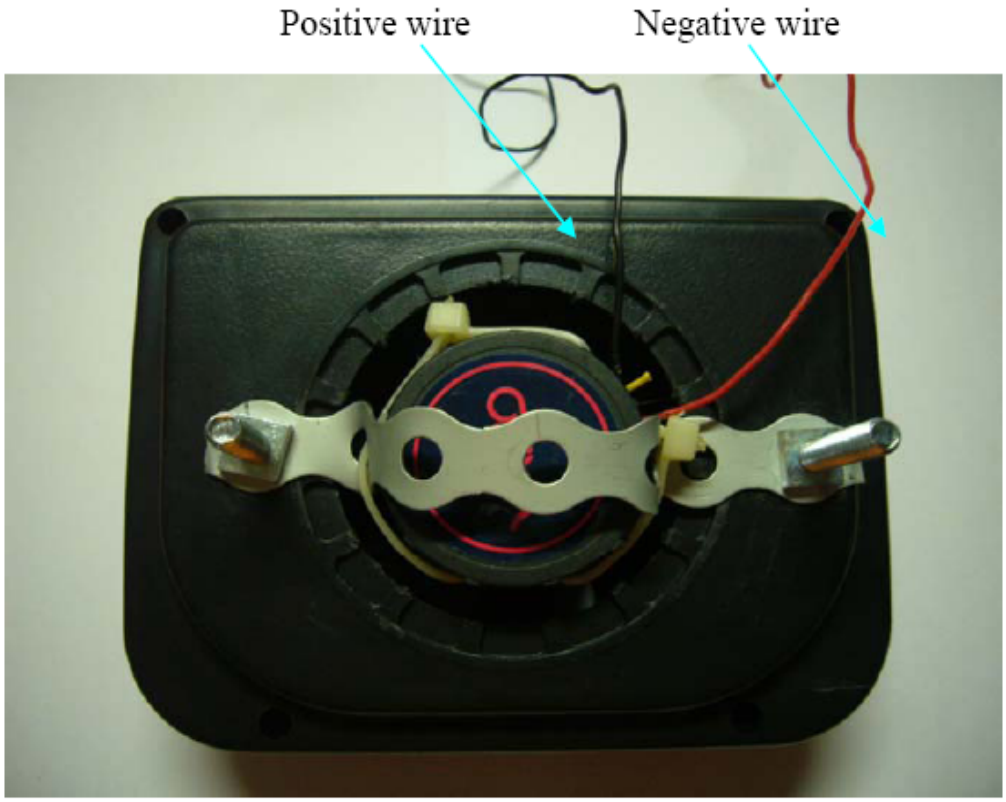

Figure 4 Improved solar car ventilator

2.5 Installation of improved ventilator

The improved solar car ventilator was designed to place on the top edge of an open window of a car. Plastic strips were used to fill the gap between the top edge of the window and the door frame as shown in the Figure 5. The strips were fitted loosely into the main unit by pushing them up into the grooves on either side of the ventilator body. The window was kept open several centimeters and the ventilator body was positioned on a suitable flat part of the window. Finally the strips were fitted along the top edge of the window. The whole ventilator was placed on the top of the window. Then, the window was closed in such a way that the ventilator can be securely held in place between the window and the door frame.

2.6 Location of solar panel

The solar panels were placed on the roof of the car so that the solar panel received maximum amount of solar irradiation and produced maximum electricity. The position of the solar panel is shown in Figure 6. The positive and negative wires of the improved ventilator were connected to the solar controller. The battery and solar panels were also connected to the solar controller separately. The schematic diagram of the improved ventilator and solar panels are shown in Figure 6.

2.7 Data collection process

The data collections were divided into 3 categories:

a) Data collection without a ventilator
b) Data collection with an existing ventilator
c) Data collection with an improved ventilator

A metallic grey color Nissan Sunny car was used as a test unit through out the investigation. The data acquisitions were done in a sunny day from 11am-4pm and the data were taken 15 minutes interval. The car was parked in an open space and exposed to the sunlight to ensure that the whole ventilation system was running at its optimum level. The solar panel, solar charger, batteries, and the improved ventilator were installed properly, and the car's side windows and doors were ensured to be fully closed. The temperatures at the front dashboard, side dashboard and back dashboard were taken using 3 digital thermocouples and their average temperatures were considered to investigate the performance. The three thermocouples were placed at the front, side, and back dashboard to take the monitor temperature at different locations.

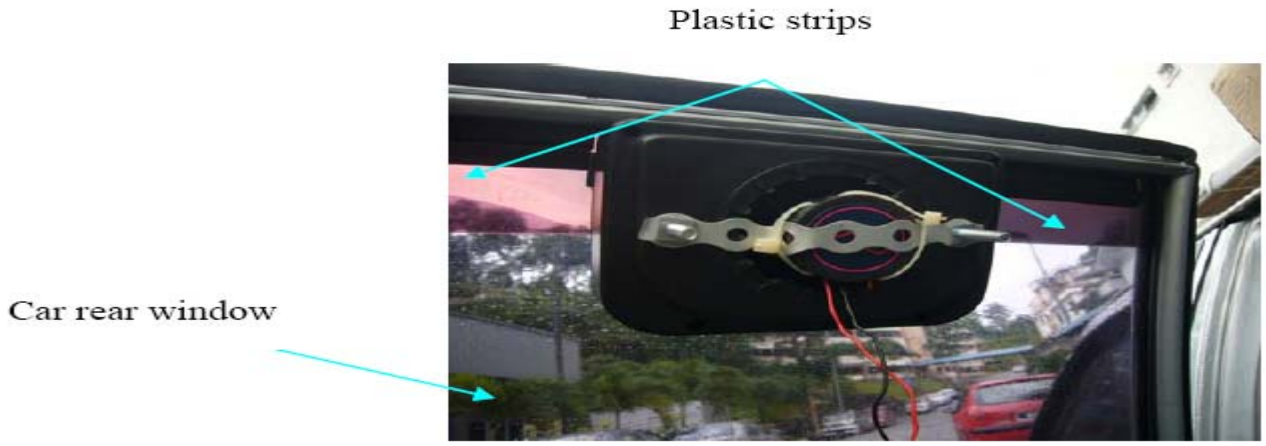

Figure 5 Improved solar car ventilator on top edge of an open window

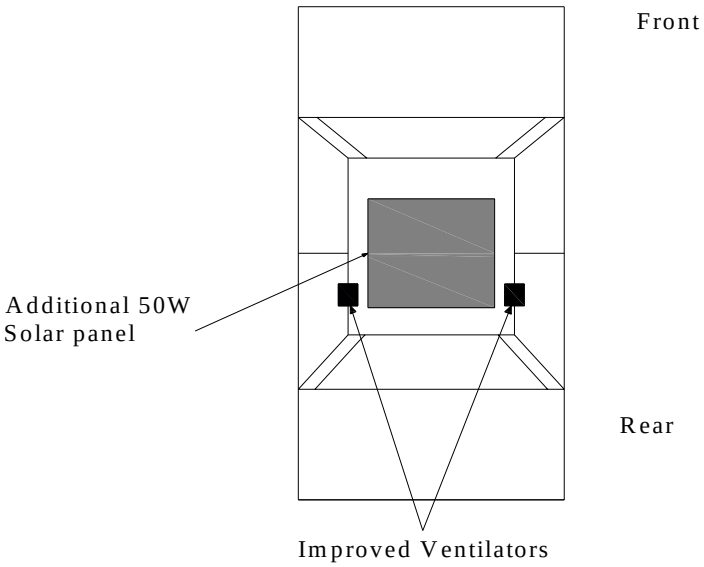

Figure 6 Position of improved ventilator and solar panel

2.8 Area of the roof and window glass.

The geometric shapes of the roof and windows shown in Figure 7(a)-(d) were used to calculate the solar heat gain inside the car compartment. The total area of window, A_g is obtained by using the geometries of window shown in Fig.7 (a)-(c).

$$A_g = \frac{1}{2}(A + C)(B) + \frac{1}{2}(G + I)(H) + 2(\frac{1}{2})(D + F)(E) \quad (1)$$

The total area of roof, A_r is obtained by using the geometric shape of Fig. 7(d).

$$A_r = (J \times K) \quad (2)$$

where $\frac{1}{2}(A+C)(B)$ is the area of front window, $\frac{1}{2}(G+I)(H)$ is the area of back window, $2(\frac{1}{2})(D+F)(E)$ is the total area of side window, and $(J \times K)$ is total area of roof.

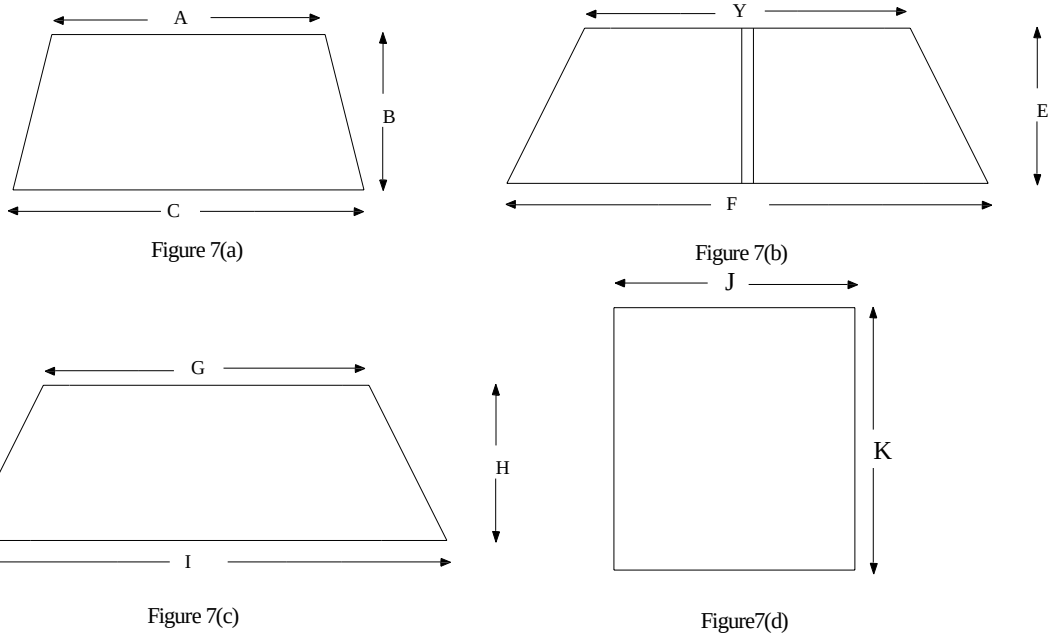

Figure 7(a)

Figure 7(b)

Figure 7(c)

Figure7(d)

Figure 7 Schematic diagrams of (a) front side (b), back (c) window and (d) roof

2.9 Formulation of heat transfer mechanism

2.9.1 Temperature inside the car compartment

The average temperature inside a car is expressed as

$$T_f = (T_{\max} + T_{\min})/2 \quad (3)$$

where $T_{\max}$ is the maximum temperature inside a car and $T_{\min}$ is the minimum temperature inside a car.

To calculate the heat gain by fluid node, the area of a fan and mass flow rate of the air enters inside the car compartment is necessary. Equations 4 and 5 were used to calculate the area of a fan and the mass flow rate respectively.

The area of fan is given by, $A_f = \pi D^2/4$ (4)

The mass flow rate is calculated by, $m = \rho Q$ (5)

The heat transfer into a car is assumed to be one dimensional and steady heat conduction. The roof is made of steel and plaster and their combined thermal resistance (combination of steel & plaster) can be written as

$$R_r = \frac{X_i}{k_i A_r} + \frac{X_p}{k_p A_r} \quad (6)$$

where $\frac{X_i}{k_i A_r}$ expresses the thermal resistance of steel and $\frac{X_p}{k_p A_r}$ expresses the thermal resistance of plaster on the roof.

It may be noted that the thermal resistance of the roof depends on the geometry and the thermal properties of the roof materials. The transition from laminar and turbulent flow depends on the surface geometry, surface roughness, free-stream velocity, surface temperature, and the type of fluid. The flow regime depends mainly on the ratio of inertia force to viscous force in fluid. This ratio is called the Reynold number, which is a dimensionless quantity, and can be expressed for external flow as

$$\mathrm{Re} = \frac{\rho V D}{\mu} \quad (7)$$

When the Reynold number is less than 2000, the flow is laminar and when the Reynold number is greater than 2000, the turbulent flow will occur.

2.9.2 Convective heat transfer coefficient

In convection studies, it is common practice to nondimensionalize the heat transfer coefficient with the Nusselt number. Nusselt number at a location for laminar flow over a flat plate (car roof surface consider flat) has been defined as (Gengel, 2004):

$$Nu = \frac{hL}{k_a} = 0.332\,\mathrm{Re}^{0.5}\,\mathrm{Pr}^{1/3} \quad (8)$$

where Pr is Prandtl number

2.9.3 Heat gain by fluid nodes

There are three modes of energy transfers for the fluid nodes: energy transfer by convection with neighboring radiative surfaces, energy transfer of mass and energy transfer by conduction between the fluid nodes. The

energy equation of fluid nodes is given by (Mezrhab and Bouzidi, 2006):

$H_f = h\ A_f\ (T_{s\ in\ fan} - T_{in}) + k_a\ A_f\ (T_{in} - T_{out}) / L + \dot{m}\ C_p\ (T_{in} - T_{out})$ (9)

where $h\ A_f\ (T_{s\ in\ fan} - T_{in})$ expresses energy transfer by fan convection,

$k_a\ A_f\ (T_{in} - T_{out}) / L$ expresses energy transfer by conduction of a fan area and

$\dot{m}\ C_p\ (T_{in} - T_{out})$ expresses energy transfer of mass.

2.9.4 Heat gain by solid nodes

The equation of energy is formulated by considering the heat exchange carried out by the windows and roof nodes. If we consider one part of the roof of the compartment; then it is composed by two nodes: internal and external. The energy equation of solid nodes is given by (Mezrhab and Bouzidi, 2005):

$H_s = h\ A_g\ (T_{s\ in\ glass} - T_{in}) + h\ A_r\ (T_{s\ in\ roof} - T_{in}) + k_g\ A_g\ (T_{s\ out\ glass} - T_{s\ in\ glass})/L_g + (T_{s\ out\ roof} - T_{s\ in\ roof}) / R_r$ (10)

where $h\ A_g\ (T_{s\ in\ glass} - T_{in})$ expresses convective heat transfer through window,

$h\ A_r\ (T_{s\ in\ roof} - T_{in})$ expresses convective heat transfer through roof,

$k_g\ A_g\ (T_{s\ out\ glass} - T_{s\ in\ glass})/L_g$ expresses energy transfer from outer window surface to inner window surface, $(T_{s\ out\ roof} - T_{s\ in\ roof}) / R_r$ expresses energy transfer from outer roof surface to inner roof surface.

2.9.5 Heat gain by radiation

Radiation heat transfer in the thermal balance of the compartment is the most complex. So it was assumed that there is no radiation emitted by the components inside the car. The radiative surfaces of the solid forming the compartment are divided into two parts roof and window. The energy equation of solid nodes is given by (Jaksic *et al*, 2003):

$H_r = \varepsilon_r\ \sigma A_r\ (T_{s\ out\ roof}^4 - T_{out}^4) + \varepsilon_g\ \sigma A_g\ (T_{s\ out\ glass}^4 - T_{out}^4)$ (11)

where $\varepsilon_r\ \sigma A_r\ (T_{s\ out\ roof}^4 - T_{out}^4)$ expresses the heat gain by radiation of roof surface and $\varepsilon_g\ \sigma A_g\ (T_{s\ out\ glass}^4 - T_{out}^4)$ expresses the heat gain by radiation through window surface.

3. RESULT AND DISCUSSIONS

3.1 Temperature inside the car

The temperature inside the car compartment is shown in Figure 8. The Figure shows that the most heated parts of the car body is the roof because most of the incident sunlight is absorbed by the roof materials. This heat is transferred from the roof to the plaster by conduction and then from the plaster to the inside environment by convection. The temperature on the glass is the lowest because the incident radiation from the sun passes through the glass into the inside compartment of the car.

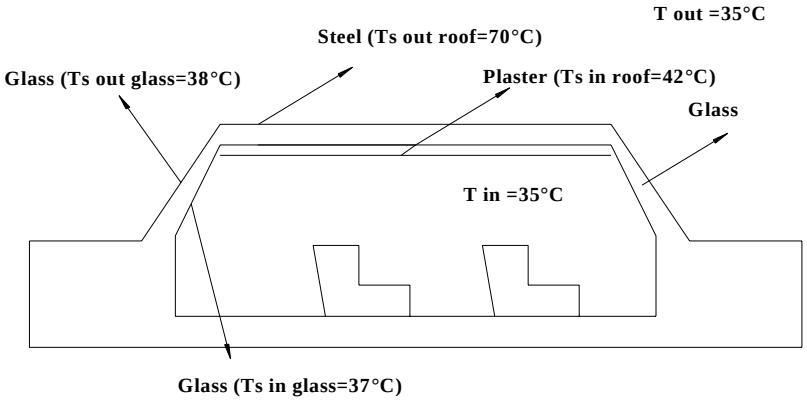

Figure 8 Temperature inside car compartment

The time based transient temperature inside the car is presented in Figure 9. The results for transient temperature inside the car compartment indicate that it is necessary to improve the ventilator in order to obtain more effective ventilation inside a car. This is not surprising, since the existing ventilator flow rate still can be increased to produce more cooling effect. The rise of temperature inside the car depends on the intensity of the radiation. On a sunny day, the temperature increases gradually at around 11.00 am and reached maximum at around 1.00 pm, then again starts to decrease as time elapses. By using existing ventilation system, highest average temperature inside a car was observed as 58.5°C at 1.00 pm. At the hottest moment, the heat gain inside a car was greater than the heat taken away by the existing ventilator. The maximum temperature observed by using

existing ventilator was only 6°C lower than the maximum temperature without using ventilator. It showed that the existing ventilator was still unable to provide a low and stable average temperature.

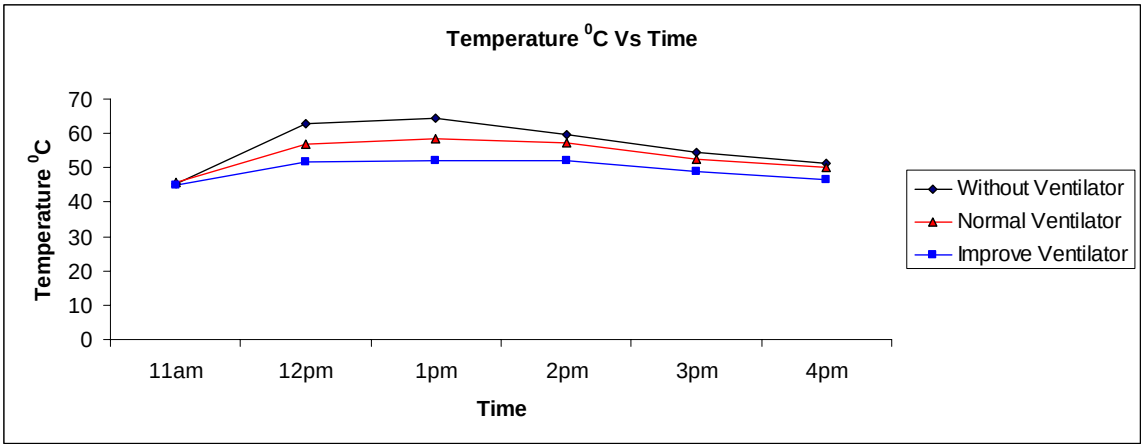

Figure 9 Temperature inside the car

Table 3 Thermal performance of existing and improved ventilator

	without ventilator	existing ventilator	improved ventilator
Average temperature at 1.00 pm	64.5 °C	58.5 °C	52.1 °C
Improvement compared to without ventilator	0 %	9.3 %	19.2 %
Improvement compared to existing ventilator	-9.3 %	0 %	10.9 %

The results in Table 3 show that the average temperature inside the car at 1.00 pm can be lowered by using the improved ventilation system. Temperatures at 1.00 pm were the main target because the temperature inside a car reaches maximum value at this time. The existing ventilation system provides 9.3 % reduction of temperature compared to a car without any ventilation system. It may be mentioned that this reduction is not enough; as the passenger would still feel uncomfortable. From the Table 3 it is obvious that the improved ventilator provide 10.9 % reduction of temperature compared to a car using existing ventilator. This improved ventilator was able to reduce 19.2 % of the temperature as compared to a car without using any ventilator.

3.2 Air circulation inside the car

The air flow rate has been found to be increased from 20 cfm to 110.5 cfm after using the improved ventilation system. The schematic diagram depicting the flow pattern of the improved ventilator is shown in Figure 10. It produced lower average temperature for passengers' comfort. In this case, two improved ventilators were placed at the rear window. Cold air entered through the air vent to the rear window, making the air inside the car to flow. So, the heat would not stay longer inside the car and the temperature increasing rate was less. The faster the air changing between the environments, the more cooling effect would be achieved inside a car. The placement of the existing ventilator's solar panel was not suitable because it was placed at the side of a car. As a result, the solar panel was not directly receiving the sunlight. To improve the efficiency of the solar panel to produce the electricity, the 50W solar panel was placed on the roof. The temperatures of front dashboard, side dashboard and back dashboard were measured. From the data analysis, it has been found that the temperature at front and back dashboard was higher than the side dashboard. Since the areas of the front and back window were slightly bigger than the side window, it allowed more sunlight to hit directly to the front and back dashboard. The dashboard having absorbed the solar radiation; it would become a heat source. It may be mentioned that the direct solar radiation greatly influence the temperature inside the car.

3.3 Heat gain of the car

Average temperature of air at 47.5°C was used to determine the air properties. The air density was used to determine the mass flow rate and specific heat and thermal conductivity were used to determine heat gain by fluid node.

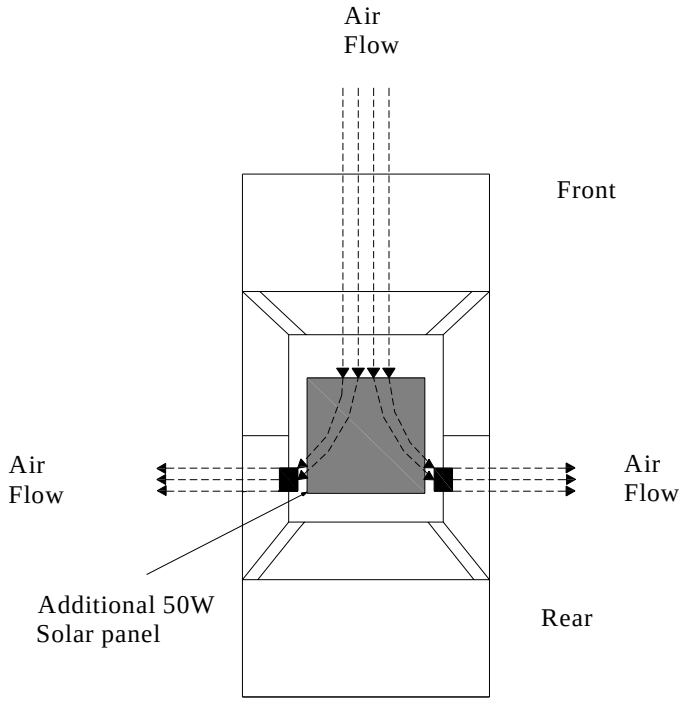

Figure 10 Air flow inside the car

Table 4 Air properties and Prandtl number

Temperature T(K)	Air density $\rho(kg/m^3)$	Specific heat C_p (J/kg.K)	Dynamic viscosity $\mu(kg/m.s)$	Thermal conductivity k_a (W/m.K)	Prandtl number (Pr)
300	1.1774	1.0057	1.8462	0.02624	0.708
320.5	1.1038	1.0071	1.9400	0.02779	0.703
350	0.9980	1.0090	2.075	0.03003	0.697

Table 5 Mass flow rate, area of fan, thermal resistance of the roof, total area of window

Mass flow rate (kg/s)	Area of fan (m^2)	Thermal resistance of the roof (^{O}c/W)	Total area of window (m^2)	Total area of roof (m^2)
0.057	3.318 X 10^{-3}	51.17	2.2928	0.912

Table 6 Heat gain by fluid nodes, solid nodes and radiation.

Heat gain by fluid nodes (W)	Heat gain by solid nodes (W)	Heat gain by radiation (W)	Total heat gain (W)
1.61x10^{-4}	6.437	24.1	30.54

Dynamic viscosity was used to determine Reynold number and Prandtl number and Reynold number and Prandtl number was used to determine the convective heat transfer coefficient. The mass flow rate, the area of fan, the area of window and the area of roof were used to calculate the heat gain, Reynold number and convective heat transfer coefficient. Heat gain inside a car was calculated in 3 ways: (a) Heat gain by fluid nodes, (b) Heat gain by solid nodes and (c) Heat gain by radiation.

Table 6 shows that heat gain by fluid nodes was 1.61×10^{-4} W, heat gain by solid nodes was 6.437 W, and heat gain by radiation was 24.1 W. It may be mentioned that heat gain by fluid was significantly lower as air has poor thermal conductivity. The heat gain by solid was significantly higher than heat gain by air because the steel is a good heat conductor and has thermal conductivity of 72.7 W/m.C. So more heat conducted from the environment into a car through the roof. Although the plaster worked as a heat insulator, it was still not effective enough to prevent the heat from getting into the car from the roof. There was only a small amount of heat conducted into a car through glasses because the thermal conductivity of the glasses is also very low (0.038 W/m.C). Most of the heat gain inside a car was through the radiation. Unlike heat gained by solid and fluid, the heat gained by radiation does not require any medium. Radiation heat transfer causes 24.1 W heat gain into the car and raises the temperature of the interior parts of the vehicle. As the interior parts of the vehicle are hot, they release heat even after the environment had started to cool. So it takes some time to cool the car even the air conditioner is switched on. Under the direct sunlight, the body and roof of the car absorbed heat and transmitted this heat by conduction into the car.

However, heat could be lost by convection and radiation from all exposed surfaces of the vehicle. Undoubtedly wind could help to increase the convection heat lost but the rate of heat lost was too low. When a car was fully closed, the air inside the car was isolated from the environment thus the hot air was not able to be released to the surrounding environment and it raises the temperature continuously. Therefore, ventilators were needed to overcome the air dankness while reducing the interior temperature to an optimum level. The increase in energy inside a car was calculated to determine the improved ventilator components' capacity such as fan power, solar panel power, solar controller capacity and battery capacity. It was calculated that 30.54 W energy need to be removed by the ventilator to maintain the car temperature same as ambient temperature. So, two Brushless DC fans with 15.6 W each were used to remove the hot air from the compartment of the car.
The total power consumption of two DC fans was 31.2W. So two solar panel of capacity 25W each were used. During the cloudy day the solar panels produce less than 50W. So 60W solar controller was used. Solar controller can automatically detect the unstable power supply and regulate the power supply to the optimum level based on the improved ventilator capacity. To complete this system, additional battery power was used to regulate the power supply. On a sunny day, 31.2 W of solar panels ran the improved ventilators and the remaining 18.8 W was used to charge 2 batteries. The total charging time of battery was estimated at 18.46 hours. During cloudy day, the improved ventilator can be operated for the next 7.2 hours by using batteries if needed.

CONCLUSIONS

In this paper the existing ventilation system was modified to increase the air flow rate and decrease the steady state temperature inside the car compartment. Two improved ventilators were built to obtain better results. The experimental results showed the improved ventilators can reduce temperature better than existing ventilator. This investigation proved that, the improved solar car ventilator can provide a comfort level higher than the existing solar car ventilator. Improved ventilator provided at least 11% reduced temperature inside a car compared to the existing ventilator. The flow rate of improved ventilator was 5.5 times higher than existing ventilator. If the flow rate of solar car ventilator is increased, the better result can be obtained for the soak temperature. It will provide greater comfort for passengers on their initial entrance to the vehicle, keeping the interior cooler. The improved ventilator is an alternative way to reduce the temperature inside a car as well as better comfort. The reduction of temperature inside the car compartment will reduce the energy consumption of the AC system. Moreover, the reduced temperature will retard the deterioration of the aesthetic look of the interior parts.

REFERENCES

A.Mezrhab and M.Bouzidi. (2006). Computation of thermal comfort inside a passenger car compartment. *Applied Thermal Engineering*, 26(14-15), 1697-1704.

C. Bureau, H. Kampf, B. Taxis-Reischl, A. Traebert, E. Mayer, R. Schwab.(2003). Method to assess thermal comfort, Vehicle Thermal Management Systems Conference Proceedings, SAE paper No. C599/005/2003, 223-233.

N.A.G. Martinho, M.C.G. Silva and J.A.E. Ramos. (2004). Evaluation of thermal comfort in a vehicle cabin, *Proceedings of the I MECH E Part D, Journal of Automobile Engineering*, 218(2), 159-166.

R.B. Farrington, R. Anderson, D.M. Blake, S.D. Burch, M.R. Cuddy, M.A. Keyser, J.P. Rugh. (1999).

Challenges and potential solutions for reducing climate control loads in conventional and hybrid electric vehicles, Vehicle Thermal Management Systems Conference VTMS4, London.

Nebojsa I. Jaksic and Cem Salahifar. (2003). A feasibility study of electrochromic windows in vehicles, *Solar Energy Materials and Solar Cells*, 79, 409-423.

K.David Huang, Sheng-Chung Tzeng, Wei-Ping Ma, Miing-Fung Wu. (2005) Intelligent Solar-Powered automobile-Ventilation System, *Applied Energy*, 80, 141-154.

J.S.M. Botterill and J.R. Williams. (1963). The mechanism of heat transfer to gas-fluidized beds, Trans Inst Chem Eng, 41, 217-230.

E.N. Ziegler, L.B. Koppel and W.T. Brazelton. (1964). Effects of solid thermal properties on heat transfer to gas fluidized bed, I&EC Fundam, 3 (4), 324-328.

Yunus A.Gengel. (2004). *Heat Transfer-A practical approach*, McGrawHill Publishers, New York.358.

Hodder, S.G., Parsons, K. The effects of solar radiation on thermal comfort. International Journal of Biometeorology Volume 51, Issue 3, January 2007, Pages 233-250.

Kaynakli, O., Unver, U., Kilic, M. (2002). Simulation of thermal comfort heating and cooling periods in an automobile compartment**.** *Proceedings of the Automotive Technologies Congress*, pp. 127-135. 24-26 June, Bursa, Turkey.